Radiation-induced attenuation in aluminum- and aluminum-thulium doped optical fibers

ANTOINE GALLET,[1,*] MATTHIEU CAUSSANEL,[1] HERVÉ DUVAL,[1] KADAR MAHAMOUD DJAMA,[1] STÉPHANE THIL,[1] JULIEN EYNARD,[1] STÉPHANE GRIEU,[1] STANISLAW TRZESIEN,[2] MICHÈLE UDE,[2] AND BERNARD DUSSARDIER[2]

[1] *PROMES-CNRS PROcédés, Matériaux et Énergie Solaire, 66100 Perpignan, France*
[2] *Université Côte d'Azur, CNRS, Institut de Physique de Nice (INPHYNI), Nice, France*
[*] *antoine.gallet@promes.cnrs.fr*

Abstract: Gamma rays induced attenuation in Al-doped and Al/Tm co-doped optical fibers is investigated in the visible and near-infrared domain up to 1 Gy. The behaviour of RIA regarding dose and dose rate is discussed. Our results reveal high sensitivities for both types of fibers at low gamma-ray doses, and also reveal that Al/Tm fibers are very promising at original interrogation wavelengths for dosimetry applications.

1. Introduction

When optical fibers are exposed to ionizing radiation, their optical attenuation increases. On the one hand, this radiation induced attenuation (RIA) has been a major concern for decades in several applications, the most iconic being probably Erbium Doped Fiber Amplifiers (EDFA) for space communications [1–5]. On the other hand, this phenomenon can be used to develop dosimeters. To do so, one can measure the RIA with an optical time domain reflectometer (OTDR). It is the mean of interrogation of the phosphorous doped silica fiber dosimeter deployed at CERN [6–8] and the germanium phosphorous co-doped fiber deployed at DESY [9]. A simpler RIA measurement configuration, based on transmission measurements with a LED and a photodiode detector has also been used for dosimetry in space [10]. Currently, there is also a strong interest in plastic fibers RIA for potential dosimeters in the medical field such as radiotherapy [11, 12].

A challenge for the RIA-based dosimetry field would be to perform highly sensitive measurements in order to address the requirements of various applications : some of which where typical dose and dose rate are weak, such as nuclear power plant decommissioning (cf. Fig. 1 of [13]) and some of which where small sizes are required, such as in-vivo dose measurements [14, 15]. The key parameter of a fiber for this type of application is its sensitivity to radiation (expressed in dB/(m·Gy)). The minimal dose that can be measured on a length unit is linked to the sensitivity of the fiber. Importance should also be given to the behavior of the RIA with respect to experimental parameters (temperature, optical power, dose rate ...). The simpler it is, the easier it is to compute the deposited dose. Another sought feature is the linearity of RIA vs. dose in the expected dose range, as it enables to have the same sensitivity during the whole lifetime of the sensor. To tackle the challenge of highly sensitive RIA-based dosimetry with silica optical fibers, it is possible to tune three parameters that have high influence on RIA : the nature of doping elements, the doping concentrations and the interrogation wavelength. Depending on the characteristics of the fiber obtained from this tuning, it can be used either for punctual or distributed sensors of various lengths.

In this work,the sensitivities under irradiation of two types of samples are investigated : Al-doped and Al/Tm co-doped fibers, in the visible and near-IR range. Al-doped fibers or bulk

glasses have already been studied under irradiation [16–19] and several color centers have already been identified experimentally from their absorption or photoluminescence signatures [20]. Regarding Al/Tm co-doped silica samples, RIA studies are mainly dedicated to the increase of their radiation resistance at doses superior to hundreds of Gy [21, 22]. Here, in-situ gamma-induced attenuation spectrum measurements for low doses (< 1 Gy), low dose rates (0.1 Gy/h or 1 Gy/h) and for both types of fibers are reported.

2. Experiments

2.1. Samples

Silica based fibers used for these experiments were prepared at Institut de Physique de Nice (INPHYNI) by Modified Chemical Vapor Deposition (MCVD). Samples lengths are 10 m ± 1%. All 6 Al/Tm co-doped fibers were drawn from the same preform. This preform was doped with the gradual-time solution doping technique [23] in order to obtain samples featuring different Tm concentrations and almost constant Al concentrations (the key point is that the concentration ratio of the two elements differs among samples). The Tm concentrations have been limited in order to have a fairly low intrinsic attenuation. The compositions of samples 11 and 12 have been measured by Electron Probe Micro Analysis (EPMA). Their thulium concentration has been confirmed by absorption spectroscopy on the Tm^{3+}: $^3H_6$ => $^3H_5$ absorption transition (peak at 1175 nm). The composition of the other samples have been deduced by absorption spectroscopy and refractivity (numerical aperture), using samples 11 and 12 as references.

The list of samples and their irradiation conditions is reported in table 1. Through the whole document, Gy(Si) is abbreviated Gy.

Table 1. Sample Table. Fibers are doped either solely with Al (n°1 to 6) or with both Al and Tm (n°7 to 12). Fibers 5, 10 and 12 have the same compositions than 4, 9 and 11 respectively but were irradiated at a lower dose rate.

Fiber n°	**[Al_2O_3]** %mol	**[Tm_2O_3]** %mol	**Dose rate** Gy/h	**Irradiation period** h
1	0.9	0	1	1
2	1.8	0	1	1
3	2.2	0	1	1
4	2.7	0	1	1
5	2.7	0	0.1	10
6	4.4	0	1	1
7	0.6	0.08	1	1
8	0.6	0.11	1	1
9	0.7	0.14	1	1
10	0.7	0.14	0.1	1
11	0.8	0.20	1	1
12	0.8	0.20	0.1	10

Typical refractive index profiles of preforms doped with Al or Al/Tm are shown respectively in Fig. 1(a) and 1(b). They have a bell-shaped graded-index profile. The core diameters of

the obtained fibers range from 7.6 µm (fiber 1) to 11.4 µm (fiber 6) for the Al-doped fibers and 7.2 µm (fiber 7) to 8.2 µm (fibre 12) for the Al/Tm co-doped ones.

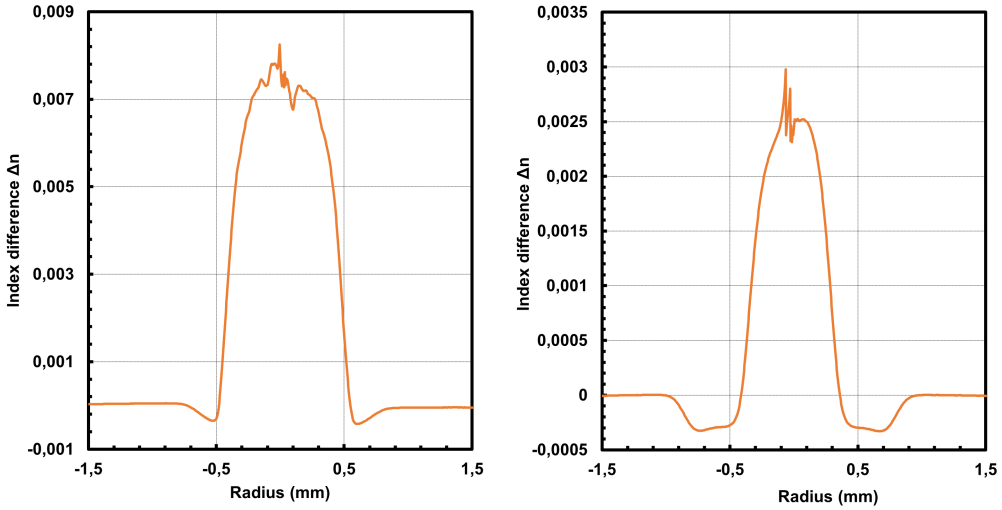

Fig. 1. Refractive index profiles of two preforms from which samples were drawn. Left graphic for an Al-doped (fibre 6) and right graphic for an Al/Tm co-doped (fibers 9 and 10)

2.2. *Irradiation and optical bench*

Samples were irradiated by a ^{60}Co gamma-rays source in the MEGA bunker at ONERA (Toulouse, France). They were spooled to a 10 cm diameter. The different dose rates were obtained by varying the distance between the source and the samples. The dose rates are estimated to be accurate within ± 10%. All irradiations have been carried out at room temperature : 22 °C to 23 °C (monitored with thermocouples).

To achieve these RIA measurements, the setup of Fig. 2 was used. A halogen bulb was chosen for its stability and wide spectral emission range. One part of the light was sent to the fiber under test (FUT) and the other part to a reference channel. The reference channel enables to take into account both the RIA of the fiber guiding light to the FUT and possible light source fluctuations. Both channels transmissions were measured simultaneously by similar spectrometers with detection range spanning from 300 nm to 1160 nm. Light transmission was monitored during irradiation and also for one hour after withdrawal of the gamma-ray source. This latter measurement enables to study a possible post-irradiation recovery.

RIA was computed with the following equation :

$$\alpha(\lambda,t) = \frac{-10}{L}\left(Log_{10}\left(\frac{S_{FUT}(\lambda,t)}{S_{FUT}(\lambda,0)}\right) - Log_{10}\left(\frac{S_{Ref}(\lambda,t)}{S_{Ref}(\lambda,0)}\right)\right) \quad (1)$$

Where : α is the RIA in dB/m, L is the FUT length in m, λ is the wavelength, t is the elapsed time since the beginning of irradiation, S_{FUT} and S_{Ref} are the spectrometer signals respectively for the FUT channel and reference channel.

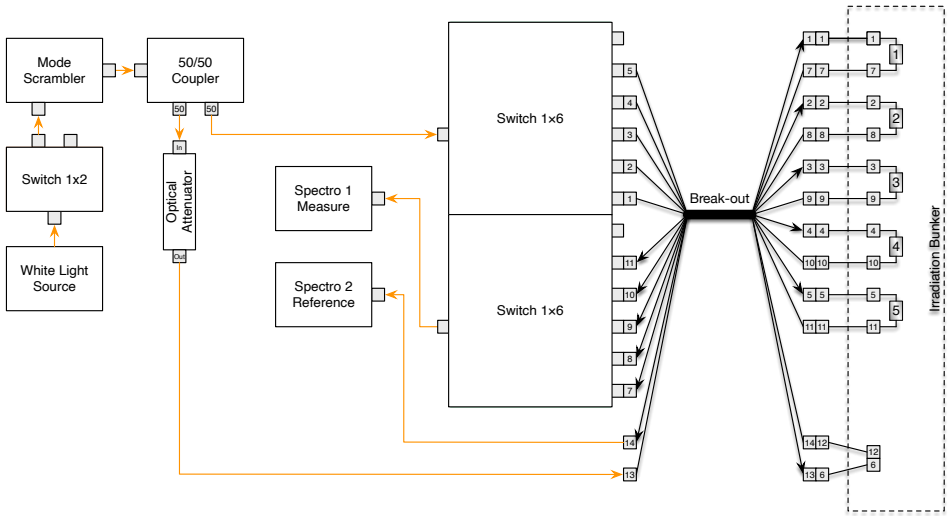

Fig. 2. Optical bench used for the RIA experiments. In this work, it is used to measure *in situ* the transmission of up to 5 FUT (rectangular frames 1 to 5) during the same irradiation. The 1x2 switch enables to perform "dark" (electronic noise) measurement. The mode scrambler stabilizes mode energy distribution before the coupler. The coupler sends 50% of the light to a 1x6 switch that guides light to the FUT. Light transmitted through the FUT is then directed to spectrometer 1 with another 1x6 switch. The fibers connecting the break-out to the FUT are radiation-hardened fibers. The other 50% of the light is sent to the reference channel. In this channel, no FUT is connected to the radiation-hardened fibers. An optical attenuator is used to prevent saturation on the detector's pixels.

3. Results

3.1. RIA spectra

The 1 Gy RIA spectra of all fibers irradiated at 1 Gy/h are shown in Fig. 3. Aluminum doped fibers have an increasing radiation sensitivity from 1160 nm to at least 600 nm. Except for the area around 550 nm to 600 nm, the RIA seems to be almost independent on concentration up to 2.7 %mol, while fiber 6 (4.4 %mol) clearly has a higher sensitivity. It indicates that doping with a high quantity of aluminum is a way to increase the sensitivity at short (<1160 nm) wavelengths for sensing applications. The absolute RIA difference between fiber 6 and any other Al-doped fiber strictly decreases from 600 nm to 1160 nm. This latter result is congruent with [24] where no significant dependency on concentration has been observed on the same type of fibers for infrared measurements (λ >1000 nm) under X-rays irradiation.

Aluminum-thulium co-doped fibers sensitivity is the highest in the range 490 nm - 620 nm. Noisy data around 465 nm and 680 nm are not taken into consideration, they are due to absorption peaks of Tm^{3+} [25]. Oddly, the absorption peak at 795 nm [26] does not lead to noisy data but to a flat RIA around this wavelength. The transmission signal is too weak to be trustworthy around 795 nm, and will not be further analyzed in the present study.

The origin of RIA in Al-doped is known to be AlOHC (Aluminum Oxygen Hole Center) for most of the spectrum, with also a contribution from AlE' center peaking in the UV [20]. Al/Tm co-doped fibers have a different spectrum shape, indicating that the Si-related and Al-related defects are not the only contributions to RIA. We believe that the Tm-related RIA in these

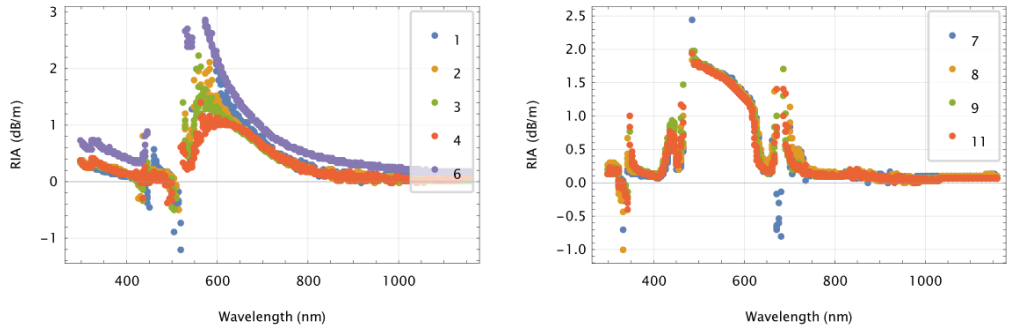

Fig. 3. RIA spectra at 1 Gy for Al-doped fibers (left) and Al/Tm co-doped fibers (right). Numbers in the legend correspond to fiber numbers in table 1. In the left graph, around 500 nm, the discontinuity and the negative values are artifacts caused by a poor signal-to-noise ratio. The transmitted light is weak in this region even before irradiation so the first term of eq. 1 is ill-defined.

fibers may arise from the reduction of Tm^{3+} to Tm^{2+} through capture of a free electron released during irradiation, in a similar fashion as photodarkening induced by UV photons [27]. Indeed, Tm^{2+} ions absorb more than Tm^{3+} ones in the whole visible domain, as revealed by cut-back measurement from Kim et al. performed on fiber doped either with Tm^{3+} or with both Tm^{3+} and Tm^{2+} [25]. Also, an increase of attenuation is visible for $\lambda > 1040$ nm in our irradiation spectra (cf. Fig. 4), which is compatible with the 1115 nm-centered absorption band of Tm^{2+} observed in their measurements.

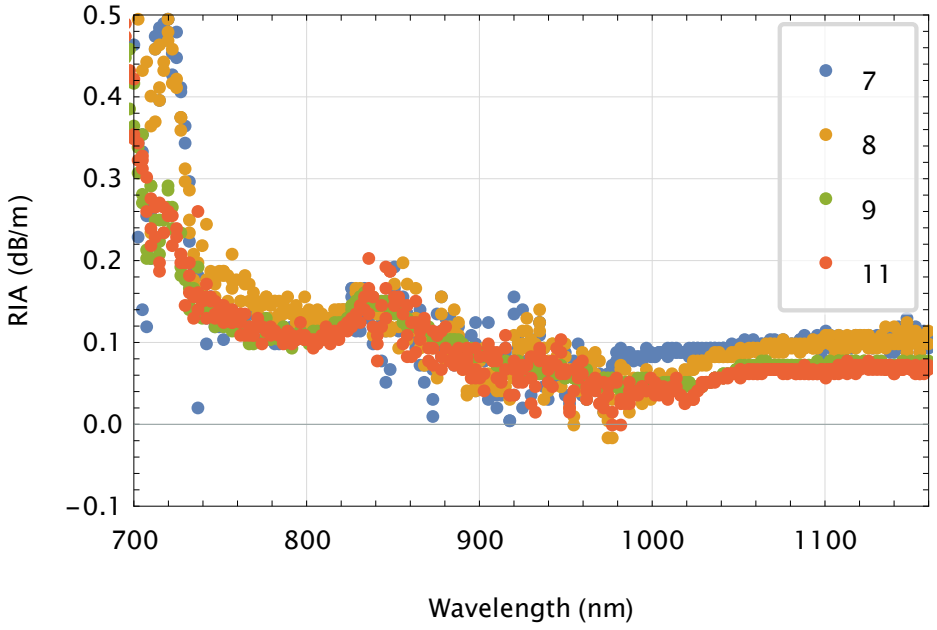

Fig. 4. Zoom on the long wavelengths of Al/Tm-doped fibers RIA spectra at 1 Gy.

3.2. Wavelengths of high sensitivity

For a dosimeter application and for both types of fibers, the research for high sensitivity is a strong incentive to operate at short wavelengths : around 490 nm for the Al/Tm co-doped ones and below 575 nm for the strongly Al-doped. RIA vs. dose at these wavelengths are reported in Fig. 5. RIA of 2.8 dB/m and 1.8 dB/m are reached at 1 Gy, by fiber 6 and by all Al/Tm co-doped fibers respectively. Even greater RIA could not be measured at 1 Gy because of the detection limit of our experimental setup. In comparison with another reported sensitive fiber, the highest sensitivity in the visible domain of the phosphorous doped fiber in [28] is less than 1 dB/(m·Gy).

The RIA vs. dose kinetic of Al/Tm-doped fibers at 490 nm and for most wavelengths in the highly sensitive range is linear, which, once again, is an important feature for sensing applications. In Fig. 5b, all Al/Tm fibers have similar RIA. This might not be the case if one performs the same measurements with significantly higher Tm^{3+} concentrations. Regarding the kinetic of Al-doped fibers, fiber 6 has a linear dose dependency at 575 nm. Also, all greater wavelengths except one feature this linear dependency (criterion $R^2 > 0.99$). On Fig. 5, it is clear, however, that all lightly doped fibers do not show a linear RIA vs. time relationship. Interestingly, the RIA kinetic of fiber 4 has been better fitted with an exponential contribution, $A \cdot \left(1 - e^{-D/D_{eq}}\right)$, similar to the one of [16], than with the classic power law, $\alpha \cdot D^{\beta}$. Sub-linear RIA curves might arise from the fact that, during irradiation, less and less pre-existing precursors are available for charge capture.

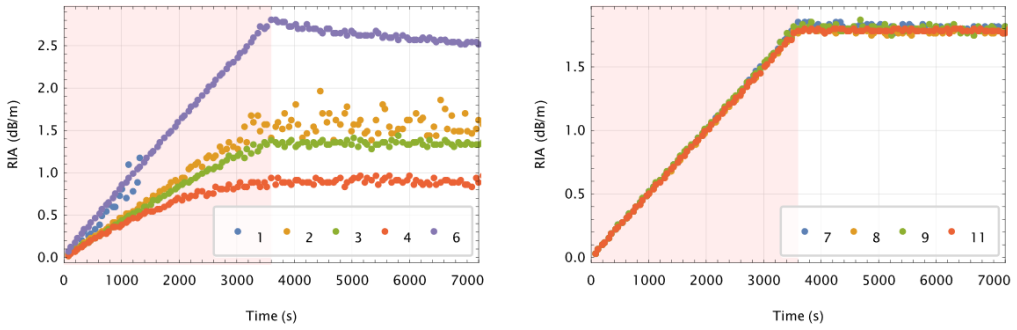

Fig. 5. RIA vs. time for Al-doped (left) and Al/Tm co-doped fibers (right) at wavelengths of high sensitivity, respectively 575 nm and 490 nm. The pink background part corresponds to irradiation, and the white one to fading. Only 1 Gy/h irradiations are shown here.

Of course, the drawback of operating at these short wavelengths is an increased intrinsic attenuation when compared to telecommunications infrared wavelengths. One can find the optimum tradeoff between higher RIA and lower intrinsic attenuation for each application by tuning the wavelength. As an example, at 850 nm, in the first telecommunications window, sensitivities of 0.4 dB/(m·Gy) for fiber 5 and higher than 0.14 dB/(m·Gy) for fibers 7 to 12 are reached. These values are still compatible with sensitive sensing.

3.3. Post-irradiation fading

At the end of irradiation, the ^{60}Co source is withdrawn and the optical transmission measurement is continued under otherwise exact same conditions. The white background part of Fig. 5 shows the post-irradiation fading for one hour. Except for fiber 6, low fading (< 5%) is observed after one hour at room temperature, indicating that stable defects are responsible for RIA at these wavelengths in both types of fibers. The fading of fiber 6 in the whole spectrum is about 10%.

When compared to lower Al concentration fibers, the higher fading percentage of fiber 6 (cf. Fig. 6a) indicates that color centers responsible for its RIA excess are less stable than AlOHC. Also, the fading curve of fiber 6 in Fig. 5 was successfully fitted (no trend in the fit residuals) with a simple exponential decay, probably arising from a single type of unstable defect. Independently from the doping concentrations and the dose rates, all Al/Tm fibers feature little fading ($\lesssim 2\%$) in the most sensitive region (cf. Fig. 6b). The similarity of the relative fading values for the different fibers of Fig. 6b is not surprising. The fibers being doped with the same elements, the color centers responsible for RIA should be the same. Thus, the relative post-irradiation fading, determined by their stability, should be the same.

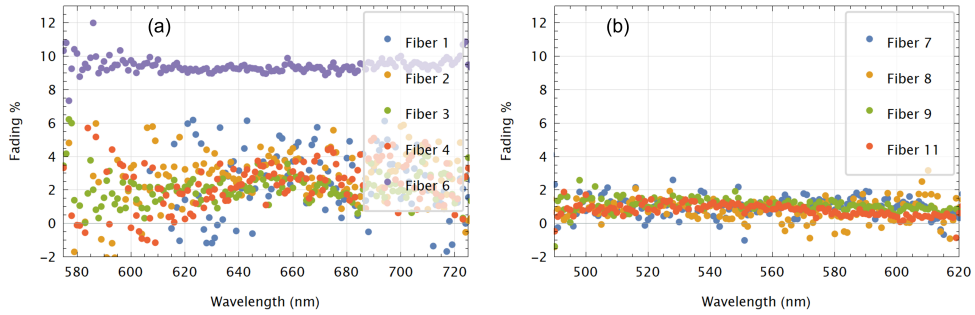

Fig. 6. % of RIA bleaching one hour after irradiation for Al-doped (left) and Al/Tm (right) doped fibers. Only 1 Gy/h irradiations are shown here.

Concerning the effect of dose rate on fading, as expected, the relative post-irradiation fading is lower for the fibers irradiated up to 1 Gy at low dose rate than for their high-dose-rate-irradiated counterparts. This is illustrated in Fig. 7. It can be explained by the fact that more thermal bleaching had occurred during the 10 h-long irradiation than during the 1 h-long one.

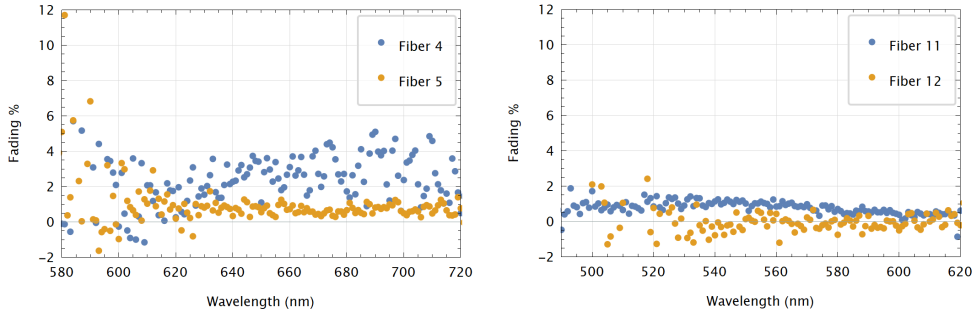

Fig. 7. % of RIA bleaching one hour after a 1 Gy irradiation with the two different dose rates for Al-doped (left) and Al/Tm co-doped fibers (right). The graphics reveal a higher fading after the irradiation at the higher dose rate (blue disks) in both cases.

3.4. Effect of dose rate

In this work, fibers 5, 10 and 12 have been dedicated to study the impact of dose rate on RIA. They are identical to fibers 4, 9 and 11 respectively. They were irradiated at 0.1 Gy/h, to estimate their degradation at sub-gray doses. Knowing the dose rate dependency is also of great interest for dosimetry. If the RIA for a given dose is independent or weakly dependent on the dose rate, it is easier to retrieve the dose from the RIA during irradiation.

Comparisons between every couple of identical fibers (4 and 5, 9 and 10, 11 and 12) reveal that the effect of dose rate is very wavelength-dependent. Moreover, for the Al-doped fiber, a clear effect of Enhanced Low Dose Rate Sensitivity (ELDRS) appears in the 575 nm - 725 nm range. This is illustrated in Fig. 8a where RIA at 1 Gy for the high dose rate divided by RIA at 1 Gy for the low dose rate is less than 1. Similarly, this effect appears at most wavelengths in the high sensitivity range of Al/Tm co-doped fiber (cf. Fig. 8b). The same conclusion holds for the ratio of fiber 9 and fiber 10 at 0.1 Gy. ELDRS in dielectrics was explained with simulations consisting of solving kinetic equations [29] or with analytical models [30]. It was previously observed in fibers with other doping elements (Er in [31], P in [32] and F in [33]), but we believe it is the first time that it is observed in Al-doped fibers. While this effect could be a flaw for dose measurement, it remains less than 20% in these ranges, which might be an acceptable error for some applications such as routine personal dose monitoring [34]. Alternatively, they could be used for narrower dose rate ranges.

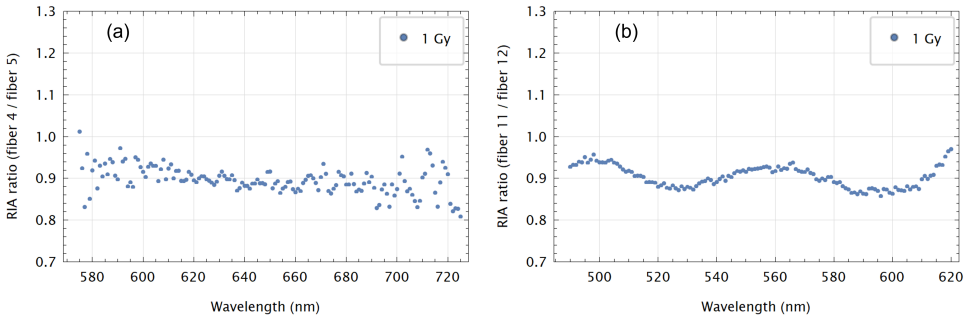

Fig. 8. RIA ratio, at 1 Gy, between high dose rate (numerator) and low dose rate (denominator) for Al-doped fibers (left) and Al/Tm-doped fibers (right).

A focus is made on wavelengths that exhibit weak RIA differences at 1 Gy between the two dose rates in Fig. 8. Comparison between RIA at 575 nm of fibers 4 and 5 reveals a very weak dependency on dose rate (cf. Fig. 9a). This result is encouraging for dosimetry. As stated before, the heavily Al-doped fiber behaves differently under irradiation than the lightly doped ones. Therefore, the observed effect on fiber 4 cannot be inferred to it and further experiments should be conducted to evaluate its dose rate dependency.

Similarly for Al/Tm co-doped fibers, a noticeable result is the very weak difference between the two dose rates sensitivities at 490 nm (cf. Fig. 9b). The difference in RIA between fibers 11 and 12 at 1 Gy is about 7% and RIA of fibers 9 and 10 are identical up to 0.1 Gy. From the similitude in RIA behaviors of all Al/Tm co-doped fibers observed in Fig. 3, 5 and 9b, it is likely that the dose rate dependency at 1 Gy is the same for the lower Tm concentrations.

3.5. Wavelengths of interest for sensing applications

In the end, Al/Tm co-doped fibers at 490 nm have the following assets for dosimetry : linear RIA vs. dose relationship at least up to 1 Gy, low fading after 1 h, weak dose rate dependency and high sensitivity of ~ 1.8 dB/(m·Gy). Hence, it seems to be a particularly interesting choice for low dose and low dose rate measurements. The computation would simply be a linear relationship between the measured attenuation α (dB) and the deposited dose D (Gy) :

$$D = \frac{\alpha}{LS} \tag{2}$$

where L is the measured length of fiber (m) and S its sensitivity (dB/(m·Gy)).

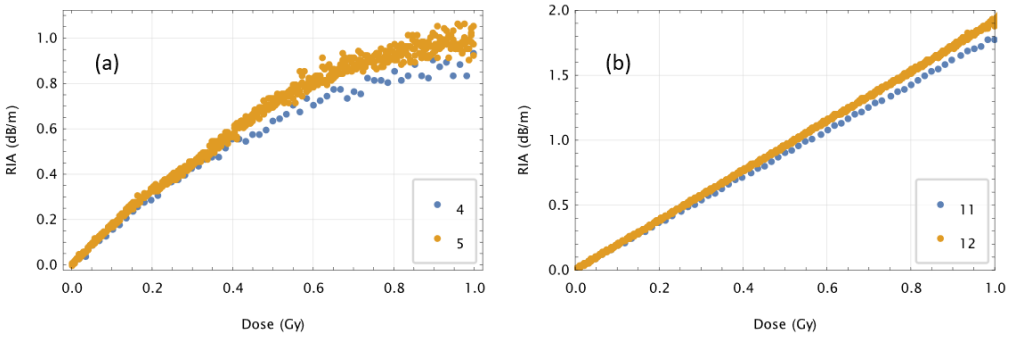

Fig. 9. RIA vs. dose for two different dose rates : 0.1 Gy/h (orange) and 1 Gy/h (blue). Fig. (a) corresponds to Al-doped fibers at 575 nm and (b) to Al/Tm co-doped ones at 490 nm. Each fiber exhibits low dose rate dependency at the selected wavelengths.

Computing dose with this simple equation would lead to less than 7% error from dose rate and only a few % more if post-irradiation fading is considered. All other wavelengths in the range 490 nm - 620 nm could also be considered for sensing applications (e.g. to reduce intrinsic attenuation or to use a given light source) as they have similar RIA behaviours. However, increasing the wavelength in this range leads to lower sensitivities and possibly slightly higher dose rate effect (cf. Fig. 8b).

While a similar statement can be made for lightly Al-doped fibers (with an exponential relationship instead of a linear one for e.g. fiber 4), post-irradiation fading observed in the heavily doped fiber leads to a more tricky problem. It seems compulsory to take it into account with a more complex model, and perform two-wavelength or multi-wavelength measurements [35, 36] in order to avoid accumulation of errors with successive irradiation/fading cycles.

4. Conclusion

RIA of Al-doped and Al/Tm co-doped fibers have been measured in the visible and near-infrared domains. From a dosimeter application perspective, this study reveals that :

1. Highly doped aluminum optical fibers could be used around 575 nm for low doses qualitative detection. However, quantitative measurements would be more complex because of post-irradiation fading.

2. Lightly Al-doped ($\leq$ 2.7 %mol) optical fibers could be used for quantitative measurements with a lower sensitivity.

3. Al/Tm co-doped fibers are suited for highly sensitive dosimetry at 490 nm at room temperature with a very simple dose computation. Other wavelengths (490 nm - 620 nm) would also be suited for dosimetry.

The wavelengths considered here are exotics but, by developing an appropriate optoelectronic system, a sensor would be feasible.

An interesting continuation of this work would be to extend the range of studied doses and dose rates in order to assess the compliance of these fibers to practical implementation requirements. Studying temperature effects would also be interesting : if the irradiation takes place at significantly different temperatures, the RIA (both during and after irradiation) can be affected. From a more fundamental point of view, no uniform dependency of RIA on Tm^{3+} concentration was observed in this study. Thus, it would also be interesting to work with smaller samples, doped with a wider range of Tm^{3+} concentrations, to clearly measure this dependency.

5. Backmatter

Acknowledgments. Portions of this work were presented at the 27^{th} International Conference on Optical Fiber Sensors in 2022, paper title : "Investigation of aluminum doped and aluminum thulium co-doped optical fibers for gamma radiation measurements".

Disclosures. The authors declare no conflicts of interest.

Data availability. Data underlying the results presented in this paper are not publicly available at this time but may be obtained from the authors upon reasonable request.

References

1. E. J. Friebele, C. C. Baker, J. S. Sanghera, M. J. LuValle, and S. Logothetis, "Erbium doped fibers for radiation tolerant, high power space laser communications," in *Free-Space Laser Communications XXXII,* vol. 11272 (SPIE, 2020), pp. 235–244.
2. G. Williams and E. Friebele, "Space radiation effects on erbium-doped fiber devices: Sources, amplifiers, and passive measurements," IEEE Trans. on Nucl. Sci. **45**, 1531–1536 (1998).
3. S. Girard, A. Laurent, E. Pinsard, T. Robin, B. Cadier, M. Boutillier, C. Marcandella, A. Boukenter, and Y. Ouerdane, "Radiation-hard erbium optical fiber and fiber amplifier for both low- and high-dose space missions," Opt. Lett., OL **39**, 2541–2544 (2014).
4. A. Ladaci, S. Girard, L. Mescia, T. Robin, A. Laurent, B. Cadier, M. Boutillier, Y. Ouerdane, and A. Boukenter, "Optimized radiation-hardened erbium doped fiber amplifiers for long space missions," J. Appl. Phys. **121**, 163104 (2017).
5. T. S. Rose, D. Gunn, and G. C. Valley, "Gamma and Proton Radiation Effects in Erbium-Doped Fiber Amplifiers: Active and Passive Measurements," J. Light. Technol., JLT **19**, 1918 (2001).
6. I. Toccafondo, Y. E. Marin, E. Guillermain, J. Kuhnhenn, J. Mekki, M. Brugger, and F. D. Pasquale, "Distributed Optical Fiber Radiation Sensing in a Mixed-Field Radiation Environment at CERN," J. Light. Technol. **35**, 3303–3310 (2017).
7. D. Di Francesca, I. Toccafondo, G. Li Vecchi, S. Calderini, S. Girard, A. Alessi, R. Ferraro, S. Danzeca, Y. Kadi, and M. Brugger, "Distributed Optical Fiber Radiation Sensing in the Proton Synchrotron Booster at CERN," IEEE Trans. on Nucl. Sci. **65**, 1639–1644 (2018).
8. D. D. Francesca, G. L. Vecchi, S. Girard, A. Morana, I. Reghioua, A. Alessi, C. Hoehr, T. Robin, Y. Kadi, and M. Brugger, "Qualification and Calibration of Single-Mode Phosphosilicate Optical Fiber for Dosimetry at CERN," J. Light. Technol. **37**, 4643–4649 (2019).
9. H. Henschel, M. Körfer, J. Kuhnhenn, U. Weinand, and F. Wulf, "Fibre optic radiation sensor systems for particle accelerators," Nucl. Instruments Methods Phys. Res. Sect. A: Accel. Spectrometers, Detect. Assoc. Equip. **526**, 537–550 (2004).
10. B. D. Evans, G. H. Sigel, J. B. Langworthy, and B. J. Faraday, "The Fiber Optic Dosimeter on the Navigational Technology Satellite 2," IEEE Trans. on Nucl. Sci. **25**, 1619–1624 (1978).
11. O. J. Olusoji, W. Kam, and S. O'Keeffe, "Radiotherapy dosimetry based on perflourinated polymer optical fibers," in *Optical Sensing and Detection VI,* vol. 11354 (International Society for Optics and Photonics, 2020), p. 113541W.
12. P. Stajanca and K. Krebber, "Radiation-Induced Attenuation of Perfluorinated Polymer Optical Fibers for Radiation Monitoring," Sensors (Basel, Switzerland) **17** (2017).
13. S. Girard, J. Kuhnhenn, A. Gusarov, B. Brichard, M. Uffelen, Y. Ouerdane, A. Boukenter, and C. Marcandella, "Radiation Effects on Silica-Based Optical Fibers: Recent Advances and Future Challenges," IEEE Trans. on Nucl. Sci. **60**, 2015–2036 (2013).
14. S. Gripp, F. W. Haesing, H. Bueker, and G. Schmitt, "Clinical in vivo dosimetry using optical fibers," Radiat Oncol Investig **6**, 142–149 (1998).
15. H. Bueker, F. W. Haesing, S. Nicolai, and B. Wolters, "Fiber optic radiation dosimetry for medical applications," in *OE/LASE '90, 14-19 Jan., Los Angeles, CA,* A. Katzir, ed. (Los Angeles, CA, 1990), p. 419.
16. C. Campanella, V. De Michele, A. Morana, A. Guttilla, F. Mady, M. Benabdesselam, E. Marin, A. Boukenter, Y. Ouerdane, and S. Girard, "Temperature Dependence of Radiation Induced Attenuation of Aluminosilicate Optical Fiber," IEEE Trans. on Nucl. Sci. pp. 1–1 (2022).
17. A. Alessi, A. Guttilla, S. Girard, S. Agnello, M. Cannas, T. Robin, A. Boukenter, and Y. Ouerdane, "Radiation Effects on Aluminosilicate Optical Fibers: Spectral Investigations From the Ultraviolet to Near-Infrared Domains," physica status solidi (a) **216**, 1800485 (2019).
18. N. Koumvakalis, "Defects in crystalline SiO2:Optical absorption of the aluminum-associated hole center," J. Appl. Phys. **51**, 5528–5532 (1980).
19. H. Hosono and H. Kawazoe, "Radiation-induced coloring and paramagnetic centers in synthetic SiO2:Al glasses," Nucl. Instruments Methods Phys. Res. Sect. B: Beam Interactions with Mater. Atoms **91**, 395–399 (1994).
20. S. Girard, A. Alessi, N. Richard, L. Martin-Samos, V. De Michele, L. Giacomazzi, S. Agnello, D. D. Francesca, A. Morana, B. Winkler, I. Reghioua, P. Paillet, M. Cannas, T. Robin, A. Boukenter, and Y. Ouerdane, "Overview of radiation induced point defects in silica-based optical fibers," Rev. Phys. **4**, 100032 (2019).

21. Y. Xing, Y. Liu, R. Cao, L. Liao, Y. Chu, Y. Wang, J. Peng, H. Li, L. Yang, N. Dai, and J. Li, "Elimination of radiation damage in Tm-doped silica fibers based on the radical bleaching of deuterium loading," OSA Continuum, OSAC **1**, 987–995 (2018).
22. Y. Jiao, C. Shao, M. Guo, M. Guzik, Y. Zhang, C. Yu, G. Boulon, and L. Hu, "Influence of Ce3+ ion on optical properties and radiation resistance in Ce3+/Tm3+-co-doped alumino-silicate glasses," Opt. Materials: X **13**, 100113 (2022).
23. J.-F. Lupi, M. Vermillac, S. Trzesien, M. Ude, W. Blanc, and B. Dussardier, "Gradual-Time Solution Doping for the Fabrication of Longitudinally Varying Optical Fibres," J. Light. Technol. **36**, 1786–1791 (2018).
24. A. Alessi, A. Guttilla, S. Agnello, C. Sabatier, T. Robin, A. Barnini, D. D. Francesca, G. L. Vecchi, M. Cannas, A. Boukenter, Y. Ouerdane, and S. Girard, "Near-IR Radiation-Induced Attenuation of Aluminosilicate Optical Fibers," physica status solidi (a) p. 2000807 (2021).
25. Y. H. Kim, U.-C. Paek, W.-T. Han, and J. Heo, "Absorption and emission properties of Tm2+ ions in germanosilicate glass fibers," Opt. Express, OE **11**, 2672–2678 (2003).
26. J. Xu, Y. Tang, Y. Yang, and Y. Hang, "High power tunable Tm3+-fiber lasers and its application in pumping Cr2+:ZnSe lasers," in *2008 Conference on Quantum Electronics and Laser Science Conference on Lasers and Electro-Optics, CLEO/QELS,* (2008), pp. 1–2.
27. J.-F. Lupi, M. Vermillac, W. Blanc, F. Mady, M. Benabdesselam, B. Dussardier, and D. R. Neuville, "Impact of cerium and lanthanum on the photo-darkening and photo-bleaching mechanisms in thulium-doped fibre," Opt. Mater. **72**, 106–114 (2017).
28. S. Girard, Y. Ouerdane, C. Marcandella, A. Boukenter, S. Quenard, and N. Authier, "Feasibility of radiation dosimetry with phosphorus-doped optical fibers in the ultraviolet and visible domain," J. Non-crystalline Solids **357**, 1871–1874 (2011).
29. R. Chen, S. W. S. McKeever, and S. A. Durrani, "Solution of the kinetic equations governing trap filling. Consequences concerning dose dependence and dose-rate effects," Phys. Rev. B **24**, 4931–4944 (1981).
30. O. Gilard, J. Thomas, L. Troussellier, M. Myara, P. Signoret, E. Burov, and M. Sotom, "Theoretical explanation of enhanced low dose rate sensitivity in erbium-doped optical fibers," Appl. Opt., AO **51**, 2230–2235 (2012).
31. B. Brichard, A. F. Fernández, H. Ooms, and F. Berghmans, "Gamma dose rate effect in erbium-doped fibers for space gyroscopes," in *Proc. of the 16th OFS,* (2003).
32. M. C. Paul, D. Bohra, A. Dhar, R. Sen, P. K. Bhatnagar, and K. Dasgupta, "Radiation response behavior of high phosphorous doped step-index multimode optical fibers under low dose gamma irradiation," J. Non-Crystalline Solids **355**, 1496–1507 (2009).
33. A. Gallet, M. Caussanel, O. Gilard, H. Duval, J. Eynard, K. M. Djama, S. Thil, S. Grieu, T. Grimaud, and A. Pastouret, "Influence of temperature and dose rate on radiation-induced attenuation at 1542 nm in fluorine-doped fibers," Appl. Opt., AO **60**, 4841–4847 (2021).
34. H. Bueker and F. W. Haesing, "Fiber optic radiation sensors," in *Optical Fibre Sensing and Systems in Nuclear Environments,* vol. 2425 (International Society for Optics and Photonics, 1994), pp. 106–114.
35. A. L. Tomashuk, M. V. Grekov, S. A. Vasiliev, and V. V. Svetukhin, "Fiber-optic dosimeter based on radiation-induced attenuation in P-doped fiber: Suppression of post-irradiation fading by using two working wavelengths in visible range," Opt Express **22**, 16778–16783 (2014).
36. H. Bueker, F. W. Haesing, and E. Gerhard, "Compensation of fading effects of radiation-induced loss by multiple wavelengths measurements," in *Fibers '92,* E. Udd and R. P. DePaula, eds. (Boston, MA, 1993), pp. 296–302.